Zuerst erschienen in: Journal of physics and chemistry of solids 58 (1997) 4, 623-637

NONISOTHERMAL TRANSPORT PROPERTIES OF α-$Ag_{2+\delta}S$: PARTIAL THERMOPOWERS OF ELECTRONS AND IONS, THE SORET EFFECT AND HEATS OF TRANSPORT

C. KORTE and J. JANEK*

Institut für Physikalische Chemie und Elektrochemie and Sonderforschungsbereich 173 der Universität Hannover, Callinstr. 3-3A, 30167 Hannover, Germany

Abstract—The ionic and electronic partial thermopowers and the Soret effect of α-$Ag_{2+\delta}S$ (low temperature phase) have been studied as functions of temperature and deviation from stoichiometry δ by means of a nonisothermal galvanic cell. From a combination of these data with results from additional measurements of the partial entropy of silver metal in α-$Ag_{2+\delta}S$, the heat of transport of silver metal is determined. The measured transport properties are discussed in respect to the defect structure and isothermal transport properties of α-$Ag_{2+\delta}S$ and information on the individual heats of transport of the mobile point defects is extracted. We observe a strong composition dependence of Q^*_{Ag} which can be explained within our formal analysis. The electronic properties can be interpreted within the model of a non-degenerate electron gas. The scattering factor of electronic defects in the statistical description of thermopower is equivalent to the electronic heat of transport in the phenomenological description

Keywords: A. chalcogenides, A. semiconductors, D. transport properties, heat of transport, thermoelectricity.

1. INTRODUCTION

The coupling of heat and matter fluxes leads to several important transport phenomena (e.g. thermal diffusion and thermoelectricity). The phenomenological description of these phenomena in the framework of irreversible thermodynamics is straightforward [1, 2] and leads to the definition of characteristic transport coefficients, relating fluxes and conjugated thermodynamic forces. An important concept in this respect is the definition of so-called heats of transport, being combinations of transport coefficients, which describe the amount of heat that is transferred by a flux of matter [1]. Despite their importance in the description of nonisothermal transport processes, both the knowledge and the understanding of the heats of transport is relatively poor, particularly in the case of ionic charge carriers in crystalline compounds. The understanding of nonisothermal electronic transport properties is far more developed, at least for the case of materials with simple electronic structures, and electronic heats of transport have been calculated for different scattering mechanisms, see Section 2.4 and Refs [3, 4].

To improve the empirical basis for a better understanding of ionic heats of transport, we started to investigate the nonisothermal transport properties of mixed conducting ionic crystals with small deviations from the ideal stoichiometry, aiming for the precise experimental determination of the heats of transport of mobile components [5–7]. In contrast to former studies of thermal diffusion in metals [8] or thermopower of purely ionic conductors (see [1], p. 427 for a short survey), the study of materials with a variable range of stoichiometry provides a major advantage. By small variations of the composition, generally both the ionic and the electronic defect concentrations and the resulting transport properties can be changed significantly and if, as in the present case, the change in composition can be controlled electrochemically and very precisely by means of suitable galvanic cells, the isothermal and non-isothermal transport properties can be studied continuously as functions of the independent thermodynamic variables. In effect, by appropriate experimental arrangements, one can determine the heat of transport of the mobile component (silver metal in the present case) on purely experimental grounds without any theoretical assumption. However, the separation of this heat of transport into the contribution of individual charge carriers can only be performed on the basis of formal arguments [9].

With respect to our experimental approach, the monoclinic low-temperature phase of silver sulfide,

*Corresponding author.

α-$Ag_{2+\delta}S$, is a material with a favorable combination of defect and transport properties [10–19]. Even at relatively low temperatures, α-$Ag_{2+\delta}S$ shows high conductivities for both electronic and ionic charge carriers. Thus, in conjunction with an extremely large thermodynamic factor, α-$Ag_{2+\delta}S$ has a chemical diffusion coefficient ($\tilde{D}_{Ag} \simeq 0.15\,cm^2\,s^{-1}$ at $\theta = 168°C$ and $\delta = 0$, see [17, 18]) which is almost as high as the chemical diffusion coefficient of the structurally disordered β-phase. The high and composition independent ionic conductivity ($\sigma_{Ag^+} = 1.56 \cdot 10^{-2}(\Omega \cdot cm)^{-1}$ at $\theta = 169°C$ [20, 10, 13]) is based on a pronounced Frenkel disorder of the cation sublattice, whereas the electronic band gap is large enough to allow for an extrinsic control of the electronic conductivity by even small variations of the metal content [13].

Since the phase field of α-$Ag_{2+\delta}S$ includes the stoichiometric composition [10], one should be able to observe both p- and n-type behaviour, depending on the exact composition. However, the mobility u_n of the electrons is considerably higher than the mobility u_p of electron holes ($\psi_e \equiv u_n/u_p \simeq 10^2$, see [13]) and thus the resulting conductivity minimum is shifted far into the p-type region, i.e. close to that boundary of the phase field which is defined by the equilibrium with sulphur. The electronic thermopower has not been measured as a function of composition and temperature to date. Data for the electronic thermopower which have been reported by Junod [16] are only of a limited value, due to the unknown composition of his specimen. No data at all for the ionic thermopower, the partial entropy of silver, the Soret effect and the heat of transport of silver are reported in the literature.

2. FORMAL CONSIDERATIONS

2.1. *The defect structure of α-$Ag_{2+\delta}S$*

α-$Ag_{2+\delta}S$ shows Frenkel disorder in its cation sublattice,

$$Ag_{Ag}^{\times} + V_i^{\times} \rightleftharpoons Ag_i^{\cdot} + V'_{Ag} \quad K_F = \exp(-\Delta G_F/RT) \tag{1}$$

with K_F in the order of $2.5 \cdot 10^{-7}$ at $\theta = 177°C$ [10], i.e. with molar fractions of intrinsic cation defects in the order of 10^{-3} ($K_F = 9 \cdot 10^{-6}$ and molar fractions of interstitials $x_i = 3 \cdot 10^{-3}$ at $\theta = 150°C$ [15]). The electronic disorder,

$$0 \rightleftharpoons e' + h^{\cdot} \qquad K_e = \exp(-\Delta G_e/RT) \tag{2}$$

is much less pronounced and, for example, leads to molar fractions of intrinsic electronic defects of $x_n = x_p = 2.4 \cdot 10^{-7}$ with $K_e = 5.8 \cdot 10^{-14}$ at $\theta = 160°C$ [10]. The pair formation enthalpy ΔH_e equals approximately 1 eV [10, 13, 19]. A variation of the metal content according to

$$Ag + V_i^{\times} \rightleftharpoons Ag_i^{\cdot} + e' \quad K_0 = \exp(-\Delta G_0/RT) \tag{3}$$

introduces additional ionic and electronic defects, but since the magnitude of metal deficiency or excess is very small ($|\delta| < 10^{-5}$), only the electronic defect concentrations are influenced significantly. The ionic transport properties remain almost constant throughout the whole range of composition.

The deviation δ from the stoichiometric composition can be defined as $\delta \equiv x_n - x_p = (c_n - c_p) \cdot V_m$, i.e. as the difference in the molar fractions of electrons and electron holes (x_n, x_p: molar fractions; c_n, c_n: molar concentrations; V_m: molar volume) and depends in a characteristic way on the chemical potential of silver [10],

$$\delta = 2K_e^{\frac{1}{2}} \cdot \sinh\left[-\frac{F}{RT}(U - U^{\#})\right] \tag{4}$$

if one assumes ideal defect behaviour (see Appendix A). In eqn (4), the chemical potential μ_{Ag} of silver is already written in terms of the EMF $U = -(\mu_{Ag} - \mu^{\circ}_{Ag})/F$ of a galvanic cell Pt|Ag|α-AgI|$Ag_{2+\delta}S$|Pt which can be used for the electrochemical measurement and control of μ_{Ag}. At the EMF $U^{\#}$ the concentrations of electrons and holes are equal, i.e. the material is stoichiometric and contains only the intrinsic concentrations of electronic and ionic charge carriers (in the following, the symbol # always denotes quantities at the stoichiometric composition).

A comment has to be made in respect to the quality of α-$Ag_{2+\delta}S$ specimens: compared to the β-phase with growth rates of several centimeters within a few days, the parabolic rate constant for the growth of α-$Ag_{2+\delta}S$ from silver metal and liquid sulphur is very small, and the growth of even small crystals takes several weeks. Thus, the $\beta \rightarrow \alpha$-transition is unavoidable if one tries to produce coarse crystalline α-$Ag_{2+\delta}S$ from the elements quickly at high temperatures. However, as Reye and Schmalzried [11] demonstrated, the phase width of α-$Ag_{2+\delta}S$ is changed significantly by the creation of dislocations and grain boundaries during the phase transition from the β- to the α-phase at 178°C. This observation is of far-reaching consequence, since most experimental studies in the past were performed on α-$Ag_{2+\delta}S$-crystals which were obtained simply from a phase transformation of β-$Ag_{2+\delta}S$. Thus, the often controversial results [11, 12] for the deviation δ from stoichiometry in α-$Ag_{2+\delta}S$ are simply due to the different concentrations of non-equilibrium defects. Even worse, with respect to a well-defined

composition of α-$Ag_{2+\delta}S$ specimens, are the studies by Junod [16] and Brüesch [19] who prepared their materials from the reaction between the powdered elements under high vacuum.

Consequently, to obtain reproducible results for the α-phase, one has to use virgin α-$Ag_{2+\delta}S$ crystals which have definitely not been subjected to a phase transformation. For the present study we used only α-$Ag_{2+\delta}S$ crystals which were grown from the elements at $\theta \approx 170°C$ and which were never transformed to the high temperature phase.

2.2. *Phenomenological description of the transport processes*

Three flux equations, describing the measurable fluxes in terms of cations Ag^+ and excess electrons e^- as building units of the crystal and of heat Q, are sufficient for the phenomenological description of all nonisothermal transport processes in α-$Ag_{2+\delta}S$ [9, 21]:

$$j_{Ag^+} = -L_{Ag^+} \cdot \left[\nabla \eta_{Ag^+} + \left(\bar{S}_{Ag^+} + \frac{Q^*_{Ag^+}}{T}\right)\nabla T\right] \quad (5)$$

$$j_{e^-} = -L_{e^-} \cdot \left[\nabla \eta_{e^-} + \left(\bar{S}_{e^-} + \frac{Q^*_{e^-}}{T}\right)\nabla T\right] \quad (6)$$

$$j_Q = Q^*_{Ag^+} \cdot j_{Ag^+} + Q^*_{e^-} \cdot j_{e^-} \quad (\nabla T = 0). \quad (7)$$

The flux of anions S^{2-} can be neglected due to the low mobility of anions in their sub-lattice. In eqns (5)–(7), η_j denotes the electrochemical potential, $\bar{S}_j$ represents the partial molar entropy and Q^*_j denotes the heat of transport of charge carrier j, respectively.

The derivation of eqns (5)–(7) from the formulation of the entropy production (according to linear irreversible thermodynamics) is straightforward [1] and the heats of transport Q^*_j are defined as ratios of the cross coefficients L_{jQ} and the diagonal transport coefficients L_{jj} (neglecting kinetic interactions between different charge carriers, i.e. $L_{jk} = 0$). The ionic and electronic fluxes contain contributions of all mobile structure elements, thus in the present case j_{Ag^+} comprises the fluxes of interstitials and vacancies, and j_{e^-} is a combination of the electron and electron hole fluxes [9].

If coupled diffusion of cations and electrons occurs ($j_{Ag} \equiv j_{Ag^+} = j_{e^-}$), whether due to a gradient of the chemical potential of one component ($\nabla \mu_{Ag} = -1/2 \cdot \nabla \mu_S$) or of the temperature, from the combination of eqns (5)–(7), only two flux equations are independent:

$$j_{Ag} = -L_{Ag} \cdot \left[\nabla \mu_{Ag} + \left(\bar{S}_{Ag} + \frac{Q^*_{Ag}}{T}\right)\nabla T\right] \quad (8)$$

$$j_Q = Q^*_{Ag} \cdot j_{Ag} \quad (\nabla T = 0) \quad (9)$$

with the definitions

$$\mu_{Ag} = \nabla \eta_{Ag^+} + \nabla \eta_{e^-} \quad \bar{S}_{Ag} = \bar{S}_{Ag^+} + \bar{S}_{e^-} \quad (10)$$

$$Q^*_{Ag} = Q^*_{Ag^+} + Q^*_{e^-} \quad (11)$$

and the transport coefficient $L_{Ag} \equiv L_{Ag^+} L_{e^-}/(L_{Ag^+} + L_{e^-})$ of silver metal. Regarding eqns (7) and (9), the heats of transport Q^*_i describe the relation between a matter flux j_i and a corresponding heat flux j_Q under the condition of a vanishing temperature gradient:

$$j_Q = Q^*_i \cdot j_i \quad (\nabla T = 0). \quad (12)$$

Explicitly, the heat of transport Q^*_{Ag} of silver metal defines the flux of heat which is driven by a unit flux of silver metal, i.e. the coupled and equal fluxes of cations and electrons, under isothermal conditions. It has to be emphasized that Q^*_{Ag} is by no means a simple quantity. It contains not only kinetic contributions given by the individual heats of transport of the mobile ionic and electronic defects (weighted by combinations of transport coefficients), but also contains thermodynamic contributions from the reaction enthalpies of local defect equilibria [9].

If a crystal with closed surfaces for matter and charge exchange is exposed to a temperature gradient, thermal diffusion takes place until the stationary state ($j_{Ag} = 0$) is reached. This stationary state is characterized by the relation

$$(\nabla \mu_{Ag})_{j_{Ag}=0} = -\left(\bar{S}_{Ag} + \frac{Q^*_{Ag}}{T}\right)\nabla T \quad (13)$$

between ∇T and the chemical potential gradient $\nabla \mu_{Ag}$ (Soret effect), i.e.:

$$\left(\frac{d\mu_{Ag}}{dT}\right)_{j_{Ag}=0} = -\left(\bar{S}_{Ag} + \frac{Q^*_{Ag}}{T}\right). \quad (14)$$

Since it is perhaps more suggestive to express the effect of a temperature gradient in terms of the chemical composition of the inhomogeneous system, one inserts the total differential $\nabla \mu_{Ag} = (\partial \mu_{Ag}/\partial c_{Ag})_T \nabla c_{Ag} - \bar{S}_{Ag} \nabla T$ into eqn (8) and obtains:

$$\left(\frac{dc_{Ag}}{dT}\right)_{j_{Ag}=0} = \frac{1}{V_m}\left(\frac{d\delta}{dT}\right)_{j_{Ag}=0} = -\frac{Q^*_{Ag}}{T} \cdot \left(\frac{\partial \mu_{Ag}}{\partial c_{Ag}}\right)^{-1}_T. \quad (15)$$

Thus, in addition to eqn (12) and due to Onsager's reciprocity relations one obtains a second interpretation for the heat of transport: Q^*_{Ag} defines the degree of thermal diffusion and stationary demixing (Soret effect) in terms of concentration gradients.

In accordance with eqn (14) one may also formulate the stationary local differences of the electrochemical potentials of both cations and electrons (setting $j_{Ag^+} =$

$j_{e^-} = 0$ in eqns (5) and (6)) which are caused by a local temperature difference and, thereby, defines the absolute partial thermopowers ϵ_i:

$$F \cdot \epsilon_{Ag^+} \equiv \left(\frac{d\eta_{Ag^+}}{dT}\right)_{j_{Ag^+}=0} - \left(\frac{\partial \mu^\circ_{Ag}}{\partial T}\right)_\delta$$

$$= -\left(\bar{S}_{Ag^+} - S^\circ_{Ag} + \frac{Q^*_{Ag^+}}{T}\right) \quad (16)$$

$$-F \cdot \epsilon_{e^-} \equiv \left(\frac{d\eta_{e^-}}{dT}\right)_{j_{e^-}=0} = -\left(\bar{S}_{e^-} + \frac{Q^*_{e^-}}{T}\right). \quad (17)$$

In eqn (16), it is already taken into account that the measurement of ionic thermovoltages can only be performed by means of ionic probes of the type Pt|Ag|AgI. Consequently, ϵ_{Ag^+} includes the partial entropy of pure silver metal.

The influence of the Q^*_i on transport processes in general can best be visualized by eqn (15). The sign and magnitude of Q^*_{Ag} determine (besides the always positive values for $(\partial \mu_{Ag}/\partial c_{Ag})_T$ and T) the degree and direction of the stationary thermal demixing, i.e. the redistribution of dissolved excess silver. An instructive example in this respect is reported by Sugisaki *et al.* [22] for the case of hydrogen in certain metals and its redistribution under the influence of a temperature gradient.

2.3. *Electrochemical measurements*

The above defined phenomenological quantities can be determined experimentally by the use of suitable galvanic cells. Thus, differences of η_{e^-} within a non-isothermal α-$Ag_{2+\delta}S$ crystal can be measured directly by the use of inert metallic probes (Pt in the present case) as the stationary electronic thermovoltage U_{el},

$$U_{el} = -\frac{\Delta \eta_{e^-}}{F} = [\epsilon_{e^-}(Ag_2S) - \epsilon(Pt)] \cdot \Delta T$$

$$= \left[\frac{1}{F}\left(\bar{S}_{e^-} + \frac{Q^*_{e^-}}{T}\right) - \epsilon(Pt)\right] \cdot \Delta T \quad (18)$$

with ϵ(Pt) representing the absolute thermopower of platinum, cf. eqn (17).

Differences of η_{Ag^+} along a nonisothermal α-$Ag_{2+\delta}S$ crystal, i.e. the ionic thermovoltage U_{ion}, can be measured correspondingly by the use of two ionic probes of the type Pt|Ag|α-AgI (cf. eqn (16)):

$$U_{ion} = \frac{1}{F}(\Delta \eta_{Ag^+} - \Delta \mu^\circ_{Ag})$$

$$= \left[\frac{1}{F}\left(S^\circ_{Ag} - \bar{S}_{Ag^+} - \frac{Q^*_{Ag^+}}{T}\right) - \epsilon(Pt)\right] \cdot \Delta T$$

$$= [\epsilon_{Ag^+}(Ag_2S) - \epsilon(Pt)] \cdot \Delta T. \quad (19)$$

The chemical potential of silver in α-$Ag_{2+\delta}S$ can be measured conveniently with a galvanic cell of the type Pt|Ag|α-AgI|α-$Ag_{2+\delta}S$|Pt. The EMF of this cell is given as

$$F \cdot U_S = -(\mu_{Ag} - \mu^\circ_{Ag}) = -RT \cdot \ln a_{Ag} \quad (20)$$

where F denotes Faraday's number, a_{Ag} represents the thermodynamic activity of silver in α-$Ag_{2+\delta}S$ and μ°_{Ag} is the chemical potential of pure silver, here used as the reference potential. In addition, by drawing an electric current across this type of cell, the silver excess of α-$Ag_{2+\delta}S$ can be changed to all values within the stability field of the material; the resulting EMF is a precise measure of the metal excess.

From the temperature dependence of the EMF of a single galvanic cell ($\nabla T = 0$), one obtains the partial molar entropy of silver, relative to the molar entropy of pure silver:

$$F \cdot \left(\frac{\partial U_S}{\partial T}\right)_\delta = -\left[\frac{\partial(\mu_{Ag} - \mu^\circ_{Ag})}{\partial T}\right]_\delta = \bar{S}_{Ag} - S^\circ_{Ag}. \quad (21)$$

Accordingly, the difference in the chemical potential of silver along a nonisothermal crystal in the stationary state (Soret effect, cf. eqn (14)) can be measured by the difference ΔU_S between the EMF of two galvanic cells at the ends of the crystal:

$$F \cdot \left(\frac{dU_S}{dT}\right)_{j_{Ag}=0} = -\left[\frac{d(\mu_{Ag} - \mu^\circ_{Ag})}{dT}\right]_{j_{Ag}=0}$$

$$= \bar{S}_{Ag} - S^\circ_{Ag} + \frac{Q^*_{Ag}}{T}. \quad (22)$$

The sum of the thermodynamic entropy $\bar{S}_i$ and the 'kinetic entropy' Q^*_i/T, which is contained in the partial thermopower (eqns (16) and (17)) and the Soret effect (eqn (22)), is often called 'entropy of transfer'.

Finally, the heat of transport of silver metal can be determined as the difference between the entropy of transfer, eqn (22), and the thermodynamic entropy, eqn (21):

$$\frac{1}{F} \cdot \frac{Q^*_{Ag}}{T} = \left(\frac{dU_S}{dT}\right)_{j_{Ag}=0} - \left(\frac{\partial U_S}{\partial T}\right)_\delta. \quad (23)$$

As can be verified by a combination of eqns (16), (17) and (22), the partial thermovoltages U_{ion} and U_{el} and the EMF difference U_S in the Soret state are not independent ($U_S = U_{el} - U_{ion}$).

2.4. *Ionic and electronic partial thermopower*

The phenomenological description of thermopower according to eqns (16) and (17) in the framework of linear irreversible thermodynamics comprises two contributions to the total thermopower: a thermodynamic part which corresponds to the partial

entropy $\bar{S}_i$ of the charge carriers and a kinetic part which corresponds to the heat of transport of the charge carriers (divided by the absolute temperature), Q_i^*/T. For electronic charge carriers, both contributions can be identified by direct comparison with the respective statistical expressions, at least in the case of the most simple electron structure based on rigid parabolic bands.

Solving the Boltzmann transport equation for this case [3, 4], the thermopower of pure n- or p-type semiconductors (see also eqn (17)) result as

$$\epsilon_{e^-} = \epsilon_n = -\frac{R}{F}\left(\frac{E_C - E_F}{RT} + \frac{5}{2} + r_n\right)$$
$$\epsilon_{e^-} \equiv \epsilon_p = \frac{R}{F}\left(\frac{E_F - E_V}{RT} + \frac{5}{2} + r_p\right) \qquad (24)$$

with E_F denoting the Fermi energy level and with E_C and E_V denoting the energies of the band edges, respectively. The terms r_n and r_p characterize the energy-dependence of the relaxation time τ of the charge carriers according to a simple power law,

$$\tau = \tau_0 \cdot E^{-r} \qquad (25)$$

and are often named *scattering factors*. With $r_n = r_p = 0$, the charge carrier motion is characterized by a constant (velocity independent) relaxation time and thus the charge carriers behave like an ideal gas in which disturbances of the distribution function relax only by collisions of the mobile particles themselves. In other words, setting $r_n = r_p = 0$, one neglects any kinetic electron-lattice interaction.

Expressing the Fermi energy in eqn (24) in terms of carrier densities N_j and state densities N_C and N_V [3] of a non-degenerate electron gas,

$$\frac{E_C - E_F}{RT} = -\ln\frac{N_n}{N_C} = \frac{3}{2}\ln\left(\frac{2\pi m_n^* kT}{h^2}\right) + \ln 2 - \ln N_n \qquad (26)$$

$$\frac{E_F - E_V}{RT} = -\ln\frac{N_p}{N_V} = \frac{3}{2}\ln\left(\frac{2\pi m_p^* kT}{h^2}\right) + \ln 2 - \ln N_p \qquad (27)$$

one finally obtains the following statistical expressions for the partial thermopowers (m_n^* and m_p^* denote the effective masses of electrons and holes):

$$\epsilon_n = -\frac{R}{F}\left[\frac{3}{2}\ln\left(\frac{2\pi m_n^* kT}{h^2}\right) - \ln N_n + \ln 2 + \frac{5}{2} + r_n\right] \qquad (28)$$

$$\epsilon_p = \frac{R}{F}\left[\frac{3}{2}\ln\left(\frac{2\pi m_p^* kT}{h^2}\right) - \ln N_p + \ln 2 + \frac{5}{2} + r_p\right]. \qquad (29)$$

These are essentially equivalent to equations for the entropy of a non-degenerate electron (or hole) gas, according to statistical theory (Sackur–Tetrode equation [23]), i.e. to

$$\bar{S}_n = R\left[\frac{3}{2}\ln\left(\frac{2\pi m_n^* kT}{h^2}\right) - \ln N_n + \ln 2 + \frac{5}{2}\right] \qquad (30)$$

$$\bar{S}_p = R\left[\frac{3}{2}\ln\left(\frac{2\pi m_p^* kT}{h^2}\right) - \ln N_p + \ln 2 + \frac{5}{2}\right]. \qquad (31)$$

for electrons and holes respectively. Comparing eqn (28) with eqn (30), two points are worth to note: the constant term 5/2 in the above expressions is part of the thermodynamic entropy and should not, as is sometimes done [24], be included into a so-called *kinetic term*. Rather, the only kinetic term which modifies the thermopower from its value predicted by the charge carrier entropy is given by the scattering factors r_n and r_p.

Thus, from a direct comparison of eqns (28) and (29) with the respective equations from irreversible thermodynamics,

$$\epsilon_n = \frac{1}{F}\left(\bar{S}_n + \frac{Q_n^*}{T}\right) \qquad \epsilon_p = \frac{1}{F}\left(\bar{S}_p + \frac{Q_p^*}{T}\right) \qquad (32)$$

we obtain for the heats of transport:

$$Q_n^* = r_n \cdot RT \qquad Q_p^* = r_p \cdot RT. \qquad (33)$$

These relations offer a reliable quantitative argument for the discussion of separate electronic heats of transport and entropies, since r_i has been calculated for various scattering mechanisms in simple electronic structures. Furthermore, from a knowledge of the electronic heat of transport and from a measurement of the heat of transport of the metal component one can now derive quantitative information on the ionic heat of transport.

According to Ref. [3], the scattering term takes e.g. a value of $r_n = -1/2$ (i.e. $Q_n^* = -1/2RT$) for the case of lattice scattering (phonon scattering) or a value of $r_n = 3/2$ (i.e. $Q_n^* = 3/2RT$) for scattering of electrons by ionized impurities, i.e. Q_n^* is relatively small in any case. Besides the absolute magnitude of the heat of transport, an important conclusion concerns the temperature dependence of the heat of transport. Depending on the scattering process, the heat of transport exhibits a more or less pronounced temperature dependence. Thus, at least from the viewpoint of electron transport theory, the assumption of temperature independent heats of transport which is often used in the analysis of ionic properties [25–27] seems to be not justified.

In the present case of a nearly intrinsic electronic conductor, the total thermopower contains contributions from both electrons and holes. The coupling of the partial electron and hole fluxes j_n and j_p leads to

the definition of the measurable flux j_{e^-} of excess electrons and the corresponding total thermopower ϵ_{e^-}. The result,

$$\epsilon_{e^-} = \frac{1}{F}\left[\frac{\Delta H_e + Q_n^* + Q_p^*}{2T} \cdot \tanh\left(\ln \alpha_e + \frac{1}{2}\ln \psi_e\right) + \frac{3}{4}R\ln\left(\frac{m_n^*}{m_p^*}\right) - R\ln \alpha_e + \frac{Q_n^* - Q_p^*}{2T}\right] \quad (34)$$

equals the sum of the partial thermopowers ϵ_n and ϵ_p, weighted by the respective transference numbers [9, 21],

$$\epsilon_{e^-} = t_n \cdot \epsilon_n + t_p \cdot \epsilon_p \quad (35)$$

In eqns (34) and (35), $t_n \equiv \sigma_n/(\sigma_n + \sigma_p)$ and $t_p \equiv \sigma_p/(\sigma_n + \sigma_p)$ denote the partial transference numbers of electrons and holes (σ_i: partial electrical conductivity), $\alpha_e \equiv x_n(\delta)/x_n(\delta = 0)$ is a dimensionless concentration variable and $\psi_e \equiv u_n/u_p$ represents the mobility ratio of electrons and holes.

The value of the heat of transport Q_e^*- of excess electrons is not immediately obvious from eqn (34). Subtracting the partial entropy $\bar{S}_{e^-}$ of excess electrons [21] (see eqns (30) and (31)),

$$\bar{S}_{e^-} = y_n \cdot \bar{S}_n - y_p \cdot \bar{S}_p = \frac{\Delta H_e}{2T} \cdot \tanh(\ln \alpha_e) + \frac{3}{4}R\ln\frac{m_n^*}{m_p^*} - R\ln \alpha_e \quad (36)$$

from the total entropy of transfer in eqn (34) finally leads to the expression

$$Q_{e^-}^* = t_n \cdot Q_n^* - t_p \cdot Q_p^* + (y_p \cdot t_n - y_n \cdot t_p) \cdot \Delta H_e \quad (37)$$

for the electronic heat of transport of a material containing both electrons and holes (with dimensionless concentration variables $y_n = x_n/(x_n + x_p)$ and $y_p = x_p/(x_n + x_p)$). In terms of the mobility ratio ψ_e and the concentration ratio α_e, eqn (37) can be rewritten as:

$$Q_{e^-}^* = \frac{\alpha_e^2\psi_e}{1 + \alpha_e^2\psi_e} \cdot Q_n^* - \frac{1}{1 + \alpha_e^2\psi_e} \cdot Q_p^* + \frac{\alpha_e(\psi_e - 1)}{(\alpha_e + \alpha_e^{-1})(1 + \alpha_e^2\psi_e)} \cdot \Delta H_e. \quad (38)$$

Different from what one would expect naively, $Q_{e^-}^*$ consists not only of the weighted contributions of Q_n^* and Q_p^*, rather it also contains an additional contribution from the reaction enthalpy of the local electron–hole equilibrium [9]. This contribution can attain an appreciable magnitude depending on the actual band gap and the mobility ratio of electrons and holes. In Fig. 1a, calculated values (see eqn (37)) for $Q_{e^-}^*$ are depicted for $\Delta H_e = 100$ kJ/mol, which equals approximately the pair formation enthalpy of α-$Ag_{2+\delta}S$ and different values of ψ_e. In Fig. 1b,

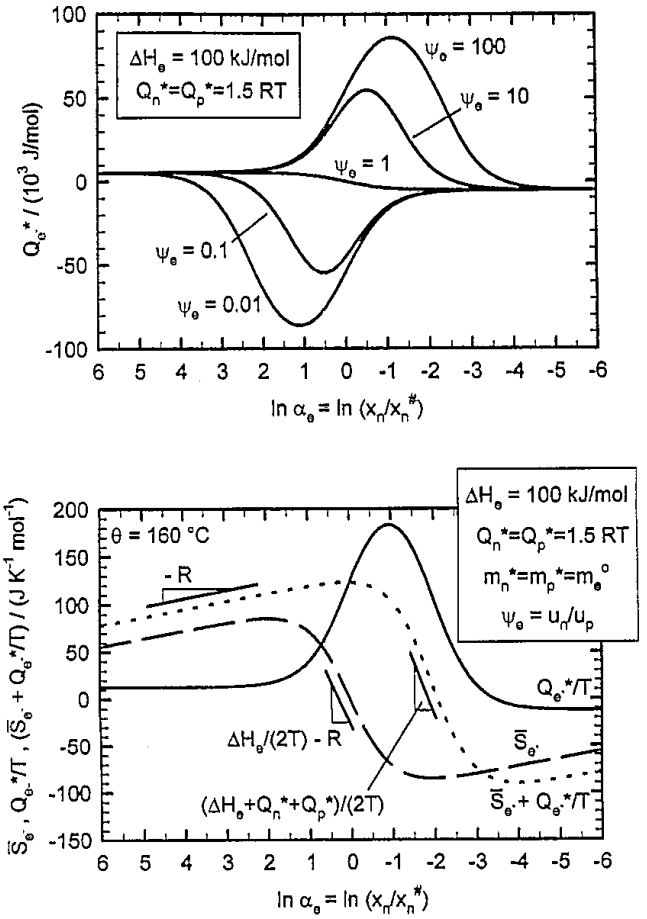

Fig. 1. (a) Electronic heat of transport according to eqn (38); parameters used: $\psi_e = 0.01$, 0.1, 10, 100; $\Delta H_e = 100\,\mathrm{kJ \cdot mol^{-1}}$, $Q_n^* = Q_p^* = 1.5 \cdot RT$, $\theta = 160°C$; (b) electronic heat of transport, electronic entropy and entropy of transfer according to eqns (38) and (36); parameters used: $\psi_e = 100$; $\Delta H_e = 100$ kJ·mol^{-1}, $Q_n^* = Q_p^* = 1.5 \cdot RT$, $m_n^* = m_p^*$, $\theta = 160°C$.

calculated values for the electronic entropy, the electronic entropy of transfer and the heat of transport are shown for a single set of parameters (according to eqns (36) and (38)).

In conclusion, the electronic heat of transport $Q_{e^-}^*$ is small and given only by the scattering terms (i.e. the heats of transport of the defects) if n- or p-type conductivity prevails significantly, i.e. in the extrinsic regions. Once both charge carriers are present, the heat of transport shows in general a pronounced extremum in its shape, depending on the actual band gap and the mobility ratio. Only for the very special case of electrons and holes with equal mobility, does the reaction term cancel. With a mobility ratio $\psi_e = u_n/u_p > 1$, does the heat of transport shows an maximum, while a mobility ratio $\psi_e < 1$ leads to a minimum of $Q_{e^-}^*$.

The subsequent experimental results for α-$Ag_{2+\delta}S$ exemplify these formal predictions for the composition dependence of the heat of transport in the vicinity of the stoichiometric composition. To our knowledge, such an experimental example has not been reported in the literature to date (results for UO_{2+x} [28], see discussion).

3. EXPERIMENTAL

3.1. *Materials*

Coarse crystalline specimens of α-$Ag_{2+\delta}S$ were grown from the elements (99.995% pure silver supplied by Heraeus GmbH, Germany; 99.999% pure sulphur supplied by Fluka Chemie AG, Switzerland) at 170°C. Since the parabolic rate constant for the growth of α-$Ag_{2+\delta}S$ is very small, we modified the conventional technique of growth into a glass capillary [25]. A piece of silver metal was exposed to liquid sulphur such that sulphide growth could take place on an area of approximately 20×5 mm. After 2 months a 4 mm thick layer of α-$Ag_{2+\delta}S$ had been grown, resulting in a $2.2 \times 2.6 \times 14.0\,mm^3$ stick of sulphide, which was separated from the metal by careful cutting.

3.2. *The galvanic cell*

Figure 2a depicts the nonisothermal galvanic cell which was used for the transport experiments. The specimen is fitted at its ends with silver iodide (99.5% AgI supplied by Riedel de Haën AG, Germany) and silver pellets as ionic electrodes for the purpose of coulometric titration and is contacted with two further and very small ionic probes at the surface near its ends. Thin platinum tubes (0.6 mm diameter) which were brought in contact with the crystal were used both as electronic probes and as containers for the thermocouples (NiCr/Ni thermocouples in an electrically isolating alumina and steel jacket, 0.35 mm diameter, Philips GmbH, Germany). The whole cell arrangement was fitted in a PTFE container and covered air tight with a temperature resistant silicone rubber after assembling, to avoid loss of sulphur by evaporation from the specimen.

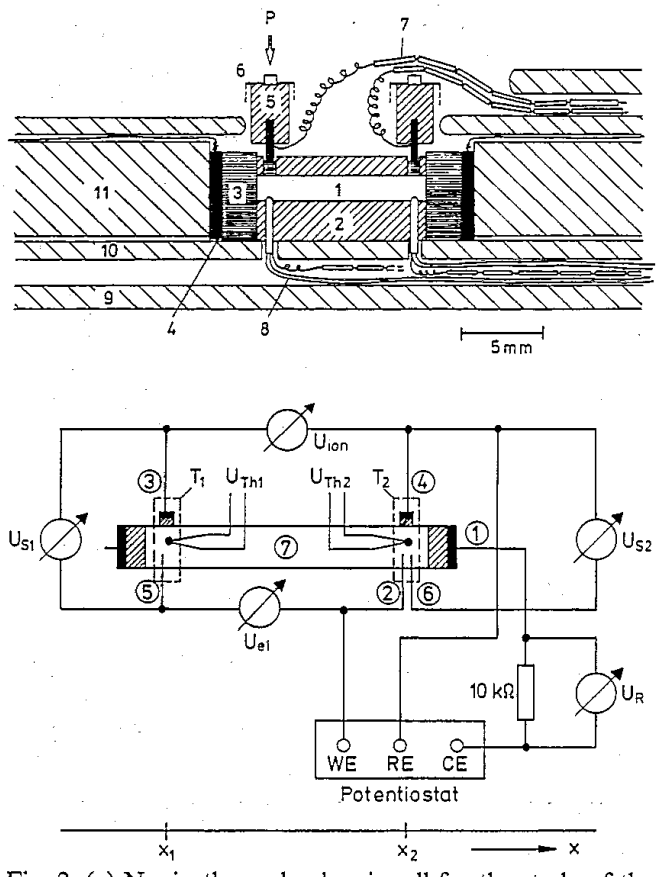

Fig. 2. (a) Nonisothermal galvanic cell for the study of the Soret effect and partial thermopowers; (b) electric circuitry of the nonisothermal galvanic cell: (1) (3) (4) ionic electrodes, (2) (5) electronic (Pt) electrodes, (7) α-$Ag_{2+\delta}S$ crystal.

The complete cell arrangement was placed in a glass tube and fixed in position with glass rods. By the use of springs, slight mechanical pressure was given to the cell. The experiments were performed in a furnace with two separate heating coils and temperature controls. Thus, the temperature on the two sides of the crystal could be controlled independently.

During all experiments, the thermopower signal of the thermocouples was stable within $\pm 2\,\mu V$, i.e. the temperature stability of the galvanic cells was better than ± 0.05 K. A temperature dependent offset of both thermocouples was observed, being always smaller than 1 K and not affecting the evaluation of the results.

3.3. *Circuitry*

Thermovoltages and EMFs were measured with a digital voltmeter (Keithley 2001), which was connected to a personal computer. The change of metal excess δ in the crystal was achieved by a coulometric titration with a potentiostat (Jaissle 5000-TB), see Fig. 2b.

3.4. *Coulometric titrations*

Before the transport experiments, coulometric titrations were performed in order to determine the range of homogeneity of the specimen and to obtain the relation between the chemical potential of silver in α-$Ag_{2+\delta}S$ and the composition of the crystal. The coulometric measurements were performed with an auxiliary galvanic cell (α-$Ag_{2+\delta}S$ specimen: diameter 5.0 mm, length 4.3 mm).

3.5. *Measurements of the partial entropy* $(\bar{S}_{Ag} - S^{\circ}_{Ag})$ *of silver metal*

Precise values for the partial molar entropy are required for the evaluation of Q^*_{Ag} from the entropy of transfer, see eqn (23), but have not yet been reported in the literature. For the measurement of the partial entropy, the temperature of an auxiliary galvanic cell was changed in steps of 1 K. The resulting changes of the EMF U were always measured twice with both increasing and decreasing temperature, i.e. in complete temperature cycles. To reduce drifts of the EMF, either due to evaporation of sulphur or due to an electronic leakage of α-AgI, we used as large samples as possible. As a result, we observed virtually

no drifts at low EMFs. At high EMFs we observed small drifts of the EMF which could easily be subtracted from the EMF changes caused by temperature changes.

3.6. *Measurement of the entropy of transfer* $(\bar{S}_{Ag} - S^{o}_{Ag} + Q^{*}_{Ag}/T)$ *of silver metal*

To perform a Soret experiment, a temperature difference $(T_2 - T_1)$ was established between the ends of the crystal by using both heating coils of the furnace. The corresponding changes of the EMFs U_{S1} and U_{S2} (i.e. the changes of the chemical potential at the ends of the crystal) due to the redistribution of the silver component were recorded vs. the temperature difference. Due to the large chemical diffusion coefficient, stationary states were generally attained within a few minutes.

Measurements were performed for various mean compositions in the temperature range between 150 and 170°C. It has to be noted that a strict evaluation of Q^{*}_{Ag} from a demixing experiment requires the integration of eqn (14). However, the actual temperature differences which have been applied ($\Delta T \leq 2\,K$) were always small enough to allow the use of arithmetic averages instead. The experimental error is less than ±5%.

3.7. *Measurement of partial thermopowers*

Simultaneously with the measurement of the entropy of transfer we measured the partial ionic and electronic thermovoltages U_{ion} and U_{el}. Since these three experimental quantities are not independent, the measurement of all three quantities provides a check on the experimental precision. The uncertainty of both thermopowers is less than ±5%.

4. RESULTS

4.1. *Coulometric titrations*

Typical experimental titration curves are depicted in Fig. 3a. The thermodynamic factor $(\partial \ln a_{Ag}/\partial \ln c_{Ag})$, calculated from the experimental results in Fig. 3a, is shown in Fig. 3b.

From a fit of eqn (4) to our experimental data we obtain values for K_e and $U^{\#}$ which are given in Table 1. The inflection point shifts to higher EMFs with increasing temperature, thus, the partial entropy of silver in α-$Ag_{2+\delta}S$ at the stoichiometric composition is higher than the entropy of pure silver (eqn (54) in Appendix A). As already observed by Reye and Schmalzried [11], the titration curves are not perfectly symmetric with reference to the inflection point, i.e. deviations from the theoretical curves (eqn (4)) occur at high EMFs. One possible experimental cause for

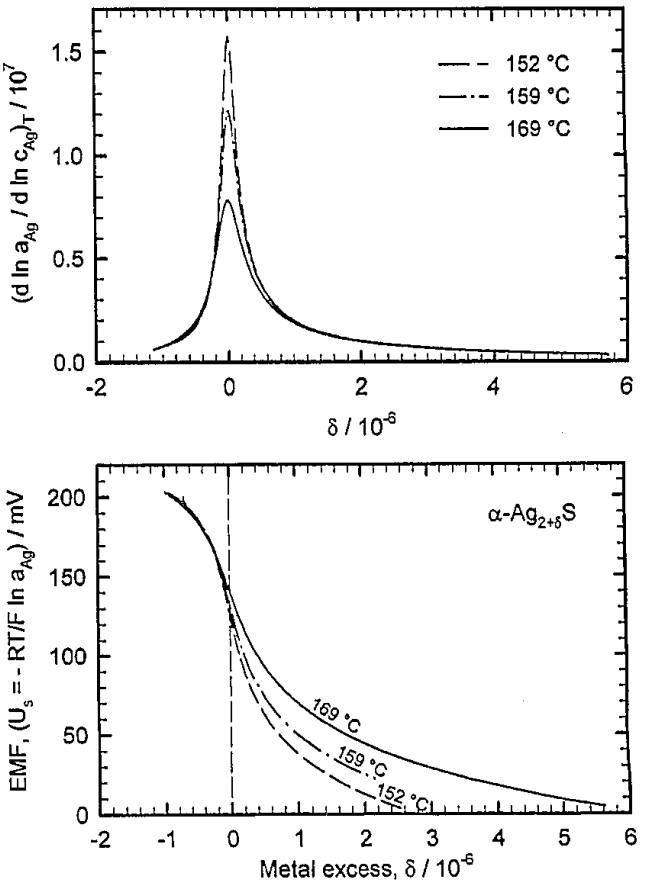

Fig. 3. (a) Results from the coulometric titration of α-$Ag_{2+\delta}S$: typical titration curves at three different temperatures; (b) results from the coulometric titration of α-$Ag_{2+\delta}S$: the thermodynamic factor at three different temperatures.

this deviation might be (electronic) leakage fluxes through the silver iodide which increase considerably at higher sulphur activities. Another reason could be copper impurities which become oxidized at higher sulphur activities.

A slight difference has been observed between titrations starting from 0 mV ($a_{Ag} = 1$) and reversed titrations starting from 200 mV ($a_{Ag} = 0.005$). The maximum error of K_e due to this effect is less than 10%, leading to an uncertainty for $U^{\#}$ of approximately 3%. In Figs 3a and b only the results of coulometric titrations with ascending EMFs are shown. All titration curves and the respective ranges of stoichiometry are in good agreement with published data [10, 13].

In conclusion, changes of the metal excess δ could be resolved to values better than $|\Delta\delta| \approx 10^{-8}$. In terms

Table 1. Numerical results of coulometric titrations on α-$Ag_{2+\delta}S$ at three different temperatures (K_e: Electronic equilibrium constant, $U^{\#}$: EMF at the stoichiometric composition, $\delta_{min} < \delta < \delta_{max}$: range of homogeneity). ΔH_e results as 97.6 kJ/mol)

θ/°C	K_e	$U^{\#}$/mV	$\delta_{min} < \delta < \delta_{max}$
152	$1.0 \cdot 10^{-14}$	118	$-1 \cdot 10^{-6} < \delta < 2.7 \cdot 10^{-6}$
159	$1.5 \cdot 10^{-14}$	128	$-1 \cdot 10^{-6} < \delta < 3.8 \cdot 10^{-6}$
169	$3.0 \cdot 10^{-14}$	135	$-1 \cdot 10^{-6} < \delta < 6.1 \cdot 10^{-6}$

Table 2. Numerical results of entropy measurements on α-$Ag_{2+\delta}S$ at three different temperatures ($U^{\#}$: EMF at the inflection point; $(\bar{S}_{Ag} - S^{\circ}_{Ag})^{\#}$: partial entropy at the inflection point; ΔH°_{e}: pair formation enthalpy)

θ/°C	$U^{\#}$/mV	$(\bar{S}_{Ag} - S^{\circ}_{Ag})^{\#}$/(J mol^{-1} K^{-1})	ΔH°_{e}/(kJ mol^{-1})
152	139	90.8	90.5
159	143	86.4	94.7
169	148	84.3	100.8

of the electron concentration, this means that changes in the order of $|N_A \cdot \Delta n_{e'}| \approx 10^{14}\,cm^{-3}$ could still be adjusted precisely.

4.2. *Partial molar entropy of silver*

In Fig. (4) the experimental results for the partial molar entropy of silver, relative to the entropy of pure silver, are shown as a function of the EMF. A second abscissa in terms of the logarithmic concentration ratio $\ln \alpha_e$ at $T = 159°C$ is depicted, in order to allow a better comparison of the results with predictions from eqn (36). The experimental error depends on the EMF but never exceeds $\pm 10\,J\,mol^{-1}\,K^{-1}$. The curves in Fig. (4) are three-parameter fits according to eqn (53), see Table 2 for the numerical results.

The temperature variation of the entropy in the investigated temperature range is negligible. As it is already obvious from the small differences between the titration curves at high EMFs (see Fig. 3a), the partial entropy becomes almost identical to the molar entropy of pure silver in the sulphur-rich phase region. At $\theta = 159°C$ an inflection point is found at an EMF of approximately 143 mV with an entropy of $(\bar{S}_{Ag} - S^{\circ}_{Ag}) \simeq 86\,J\,(K\,mol)^{-1}$. This inflection point shifts to higher EMFs with increasing temperature. According to eqn (53), the inflection point should be situated at the stoichiometric composition. In slight contrast to this, the EMF value at the entropy inflection point is always by 10% higher than the EMF at the inflection point of the coulometric titration curves. The slope of the partial entropy vs the EMF should take a constant value of F/T for small EMFs ($\alpha_e \gg 1$) if the excess silver is completely ionized, according to eqn (53) in Appendix A. As indicated in Fig. 4, the experimental data fit perfectly to this slope.

The entropy S°_{Ag} of pure silver metal in the investigated temperature range runs from 51.7 to 52.7 $J \cdot (K\,mol)^{-1}$ [29], thus the partial entropy $\bar{S}_{Ag}$ of α-$Ag_{2+\delta}S$ at $\delta = 0$ takes values between 137.0 and 142.5 $J \cdot (K\,mol)^{-1}$ in the investigated temperature range. $\bar{S}_{Ag}$ equals the sum of the partial entropies of ions and electrons, i.e. $\bar{S}_{Ag} = \bar{S}_{Ag^+} + \bar{S}_{e^-}$. Corresponding to the high intrinsic disorder of the cation sublattice, the ionic entropy is virtually composition independent and from $\bar{S}_{Ag} \simeq \bar{S}_{e^-} + \text{const.}$ we obtain

$$d\bar{S}_{Ag} \simeq d\bar{S}_{e^-} \qquad (T = \text{const.}) \qquad (39)$$

i.e. the composition dependence of $\bar{S}_{Ag}$ is exclusively determined by the electronic entropy. However, since neither the constant ionic contribution nor the electronic contribution to the partial entropy of silver metal is accessible by experimental means, one cannot separate the partial entropies.

4.3. *The entropy of transfer* $(\bar{S}_{Ag} - S^{o}_{Ag} + Q^{*}_{Ag}/T)$

In Fig. 5, measured values for the (relative) entropy of transfer $(\bar{S}_{Ag} - S^{\circ}_{Ag} + Q^{*}_{Ag}/T)$ of silver metal are

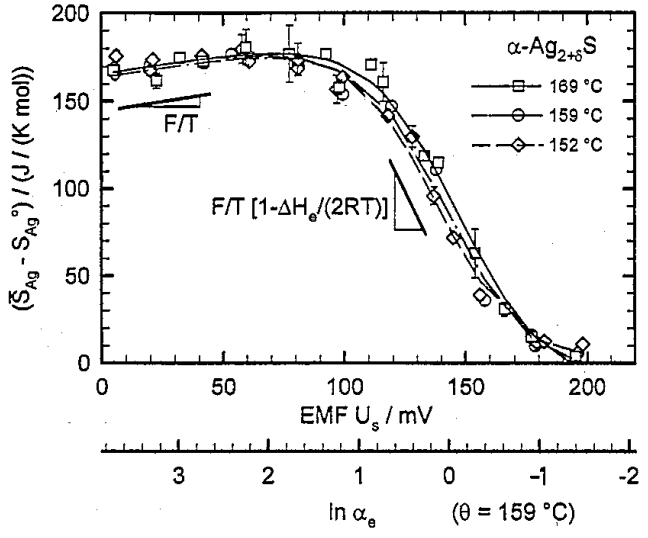

Fig. 4. Measured values for the relative partial molar entropy of silver metal in α-$Ag_{2+\delta}S$ as a function of EMF and temperature. A second abscissa denotes the concentration ratio α_e.

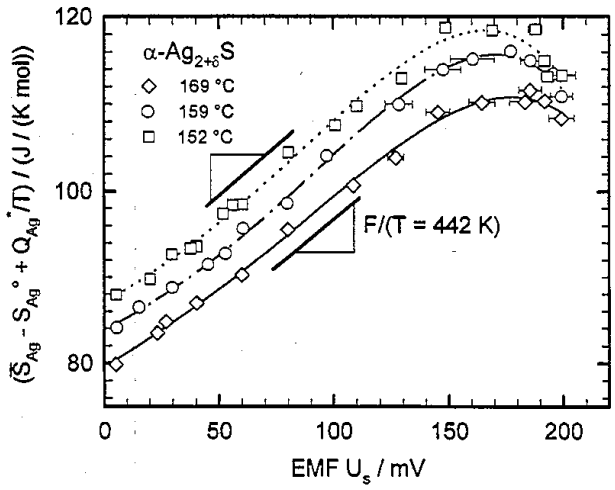

Fig. 5. Measured values for the entropy of transfer of silver metal $(d\mu_{Ag}/dT)_{j_{Ag}=0}$ as a function of EMF and temperature.

shown for three different temperatures as a function of the EMF. The experimental resolution is quite high, all data are perfectly reproducible and the experimental error is less than ±3%. In contrast to the purely thermodynamic entropy data in Fig. 4, the entropy of transfer shows a distinct temperature dependence, i.e. it decreases with increasing temperature. Since data are only available for three temperatures, this dependence will not be further discussed. Compared to $(\bar{S}_{Ag} - S^{\circ}_{Ag})$, the entropy of transfer shows a completely different composition dependence which reflects directly the influence of the heat of transport of silver metal (see below).

4.4. *The partial ionic thermopower*

In Fig. 6, the measured ionic thermopower is depicted. It is virtually independent of both temperature and composition. The experimental error amounts to approximately ±3%. A slight tendency for a decrease in ϵ_{Ag^+} with increasing temperature is observed, but is too small to be resolved. The same is true for the compositional dependence. A slight decrease of the ionic thermopower seems to take place in both directions of metal deficit and excess, thus suggesting a maximum around the stoichiometric composition. Again, this effect is too small to be analyzed.

The redistribution of the silver excess in a temperature gradient leads to a change of the partial thermopowers. Since the stationary state was always reached very quickly we were not able to detect the time variation of the thermopowers reliably, i.e. the measured data represent the thermopower in the stationary state. A direct observation of the metal redistribution via a time-resolved measurement of the ionic thermopower, however, is possible for α-$Ag_{2+\delta}Se$ [30] which possesses a much smaller chemical diffusion coefficient.

4.5. *The partial electronic thermopower*

In Fig. 6, the partial electronic thermopower which shows exactly the same composition and temperature dependence as the entropy of transfer, is shown too. One has to conclude that, besides a constant ionic contribution, the electronic properties dominate the entropy of transfer.

As already stated, the hole mobility u_p is considerably smaller than the electron mobility u_n and thus only the electronic part of the characteristic S-shaped thermopower curve can be observed within the stability field of α-$Ag_{2+\delta}S$. As expected, the slopes of the linear parts equal R/F if ϵ_{e^-} is plotted vs $-\ln \alpha_e$. In Fig. 6, the average EMF ($U_S = -RT/F \cdot \ln a_{Ag}$) of the cell is chosen as the abscissa. Thus, the corresponding slopes of the n-branches equal $1/T$ (see marks in Fig. 6).

4.6. *The heat of transport of silver metal*

Subtracting the thermodynamic entropy data, $(\bar{S}_{Ag} - S^{\circ}_{Ag})$, from the data for the entropy of transfer, $(\bar{S}_{Ag} - S^{\circ}_{Ag} + Q^{*}_{Ag}/T)$, we obtain the heat of transport of silver metal, see Fig. 7. It shows a strong dependence on the metal content, i.e. on the dominant type of electronic defect. In the silver excess region (low EMF), which shows predominant n-type conductivity, the heat of transport takes a constant value of approximately $-37\,kJ \cdot mol^{-1}$. On passing the stoichiometric composition (between 120 and 140 mV, depending on the temperature), the heat of transport increases appreciably, crosses zero and again reaches a plateau at approximately $+45\,kJ \cdot mol^{-1}$. Thus, within the narrow composition range from $\delta \simeq -1 \cdot 10^{-6}$ to $\delta \simeq 6 \cdot 10^{-6}$ the measured heat of transport varies drastically, changing by approximately $82\,kJ \cdot mol^{-1}$ and even showing a sign reversal.

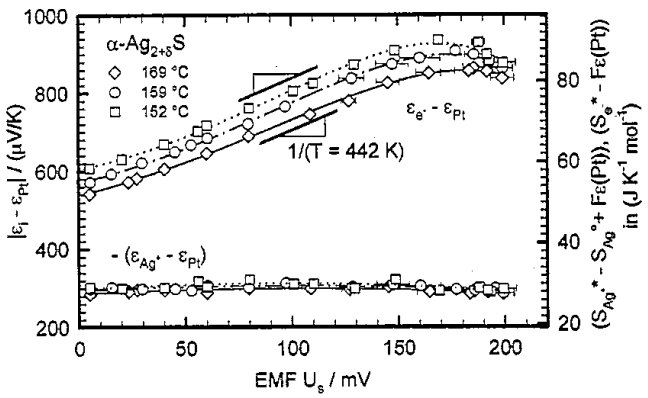

Fig. 6. Measured values for the electronic and ionic thermopower (electronic and ionic entropy of transfer) as functions of EMF and temperature.

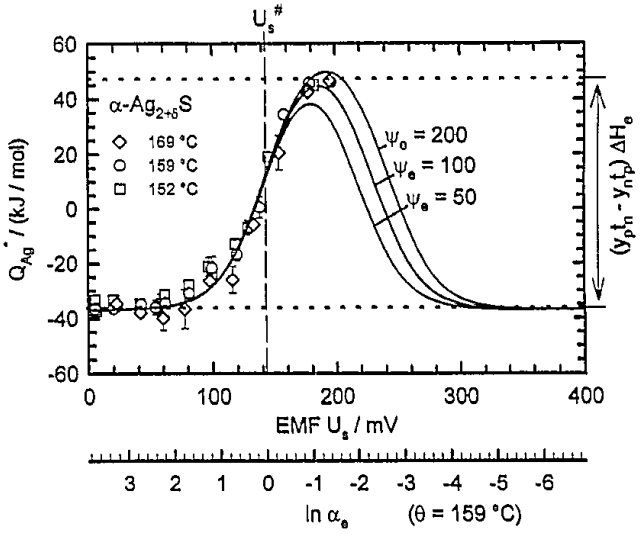

Fig. 7. Measured values for the heat of transport of silver metal as a function of the silver activity.

Q^*_{Ag} is determined as the difference of two measured quantities and its experimental error equals approximately ±5 kJ/mol, increasing slightly in the direction of higher EMFs. In Fig. 8, all experimental data at $\theta = 159°C$ are depicted together.

5. ANALYSIS AND DISCUSSION

In the following we try to advance a coherent interpretation for the observed transport properties and to give an explanation for the strong composition dependence of the heat of transport of silver metal. The underlying formal analysis is mainly based on two assumptions: (1) the electronic defect structure of α-$Ag_{2+\delta}S$ can be described in terms of free and non-degenerate charge carriers in rigid parabolic bands; (2) ionic transport properties do not change as a function of the defect concentration. In view of our experimental results, both assumptions are well founded.

5.1. *Electronic properties*

From an analysis of the titration curves we obtain the equilibrium constants K_e at three different temperatures and evaluate the electron–hole formation enthalpy $\Delta H_e \simeq 97.6$ kJ/mol for the average temperature (see Table 1). Both the values for K_e and the value for ΔH_e are in good agreement with values reported by Schmalzried [10] and Reye [11]. The values of Bonnecaze [13] for K_e are smaller than our values by one order of magnitude. The enthalpy value of

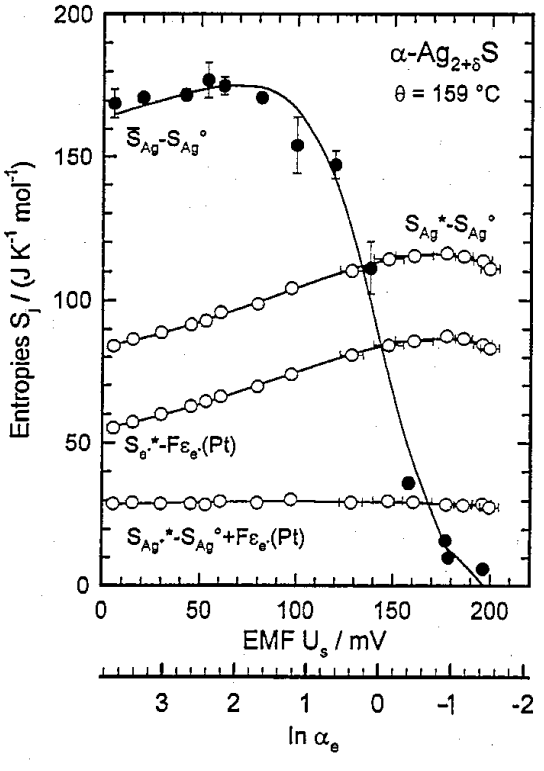

Fig. 8. Measured values for the electronic and ionic entropies of transfer, the entropy of transfer of silver metal and the entropy of silver metal at $\theta = 159°C$.

$\Delta H_e = 97.6$ kJ/mol coincides with those values which we determine from the analysis of entropy measurements (see Table 2).

Data for the electronic band gap from optical measurements are reported by Brüesch and Wullschleger [19]. They give the relation $\Delta E_B = [1.35–1.5 \times 10^{-3}\ (T/k)]$ eV for the band gap which results in values of $\Delta E_B = 0.713$ eV (0.702 and 0.687 eV) at $\theta = 152°C$ (159 and 169°C). Thus, the optical band gap is considerably smaller (70%) than the thermodynamic electron–hole formation enthalpy. Even more interesting is the different temperature dependence of ΔE_B and ΔH_e: whereas the band gap decreases with increasing temperature, the pair formation enthalpy increases with increasing temperature.

Since ΔH_e is in the order of 1 eV, the intrinsic concentration of electronic charge carriers is quite small and one may infer non-degeneracy inspite of the different effective masses of electrons and holes. As a simple criterion of degeneracy, the distances of the band edges to the Fermi level have to be sufficiently large ($(E_C - E_F)/kT \geq 2$ and $(E_F - E_V)/kT \geq 2$) [4]. Assuming simple spherical energy surfaces, the densities of states N_C and N_V (for electrons or holes with an effective mass $m^* = m_e^0$) equal $4.34 \cdot 10^{19}$ cm^{-3} at 160°C. According to the results of the coulometric titration, the concentrations of electrons or holes at this temperature does not exceed 10^{17} cm^{-3} ($\delta = 6.0 \times 10^{-6}$, if $a_{Ag} = 1$ at 169°C). And thus, using the relations $(E_C - E_F)/kT = \ln(N_C/N_n)$ and $(E_F - E_V)/kT = \ln(N_V/N_p)$ in eqns (26) and (27), the above given criteria for non-degeneracy are fulfilled for the whole range of composition.

The mobility ratio ψ_e of electrons and holes is not known very precisely and considerable disagreement exists in the literature. Bonnecaze *et al.* [13] determined the electronic partial conductivity as a function of temperature and composition indirectly by subtraction of the measured ionic dc-conductivity from the measured total ac-conductivity. They found that the minimum of the electronic conductivity is shifted considerably into the p-region. At high temperatures the minimum was not found within the phase field. Without denoting the corresponding temperature, Bonnecaze reports a value of $\psi_e = 109$ with $u_n = 60$ cm^2 (Vs)$^{-1}$ and $u_p = 0.55$ cm^2 (Vs)$^{-1}$. In view of inconsistencies in the experimental conductivity data, we will disregard this analysis. Junod [16] reports a value $\psi_e = 3.34$ for the mobility ratio of 100°C ($u_n = 63.5$ cm^2 (Vs)$^{-1}$, $u_p = 19$ cm^2 (Vs)$^{-1}$). Agreement thus exists for the electronic mobility, but the hole mobilities differ by a factor of 30. For the analysis of the heat of transport it is at this point sufficient to know that the mobility ratio is larger than 1.

5.2. *Ionic properties*

The concentrations of intrinsic ionic defects (interstitials and vacancies) are much higher than possible concentrations of additional extrinsic defects. Thus, as expected, the ionic partial conductivity α_{Ag^+} [20] and thermopower ϵ_{Ag^+} (see Fig. 6) are independent of the metal excess δ. As a consequence, we can safely assume that the partial ionic entropy $\bar{S}_{Ag^+}$ and heat of transport $Q^*_{Ag^+}$ are constant at all compositions. A separation of the ionic thermopower into its two parts $\bar{S}_{Ag^+}$ and $Q^*_{Ag^+}$ is not possible, and thus, we cannot extract any reliable quantitative information on the absolute magnitude of $Q^*_{Ag^+}$ at this point. From temperature dependent (four point) measurements of the ionic conductivity, we determine the activation energy of the cations interstitials as $E_{a,i} = 5.2\,\mathrm{kJ \cdot mol^{-1}}$.

5.3. *Heats of transport*

Taking the above considerations into account, the interpretation of the heat of transport data as a function of the metal excess is straightforward. Since the ionic contribution $Q^*_{Ag^+}$ is assumed to be constant, the composition dependence has to be explained by the electronic contribution $Q^*_{e^-}$. Referring to eqn (37) and the magnitude of the scattering terms, one can assume that the electronic heat of transport is small in the extrinsic regions (for lattice scattering: $Q^*_n = -1/2\,RT \simeq -1.8\,\mathrm{kJ \cdot mol^{-1}}$, for ionized impurity scattering: $Q^*_n = 3/2RT \simeq 5.4\,\mathrm{kJ \cdot mol^{-1}}$). Regarding the plateau of $Q^*_{e^-}$ at low EMFs, i.e. the n-type region, this leads to the conclusion that $Q^*_{Ag^+} \simeq Q^*_{Ag} = -37\ \mathrm{kJ \cdot mol^{-1}}$, independent of the actual scattering mechanism.

According to eqn (38), $Q^*_{Ag^+}$ is composed of three parts: two including the heats of transport Q^*_i and Q^*_v of interstitials and vacancies and one reaction term including the Frenkel enthalpy ΔH_F. A value for $\Delta H_F = 138\,\mathrm{kJ \cdot mol^{-1}}$ has been determined by Jost [31] from measurements of the heat capacity. With a value of the mobility ratio of interstitials and vacancies which can be taken from an experimental study by Weiss [15] ($\psi_i = u_i/u_v \simeq 4$), the reaction term of the ionic heat of transport can be approximated as $0.3 \cdot \Delta H_F = 41.4\,\mathrm{kJ \cdot mol^{-1}}$ ($\alpha_i \simeq 1$). Thus, we obtain the following result for the heats of transport of interstitials and vacancies:

$$t_i \cdot Q^*_i - t_v \cdot Q^*_v = 0.8 \cdot Q^*_i - 0.2 \cdot Q^*_v \simeq -78.4\,\mathrm{kJ/mol}. \tag{40}$$

Recalling the relation $Q^*_j = U^*_j - \bar{H}_j$ between the heat of transport and the energy of transport [20], we obtain from eqn (40):

$$0.8 \cdot U^*_i - 0.2 \cdot U^*_v \simeq -78.4\,\mathrm{kJ/mol} + 0.5 \cdot \Delta H_F = -9.4\,\mathrm{kJ/mol} \tag{41}$$

if we assume that $\bar{H}_i \simeq \bar{H}_v \simeq 0.5 \cdot \Delta H_F$. This assumption is a very rough estimate and thus eqn (41) is less reliable than eqn (40).

A more or less close relation between the heat of transport and the activation energy for the thermally activated defect jumps has been assumed by several authors [32]. Often, the relations $Q^*_i \leq E_{a,i}$ and $Q^*_v \leq -E_{a,v}$ were discussed, i.e. one assumes that the activation energies of ions (either in the interstitial or the regular cation sublattice) are identical to their heats of transport. Bonnecaze *et al.* [13] obtain values for the activation energy of interstitial jumps, $E_{a,i} = 13.0\,\mathrm{kJ/mol}$ and of vacancy jumps,* $E_{a,v} = 33.8\,\mathrm{kJ/mol}$, from conductivity measurements on α-$Ag_{2+\delta}S$. Own conductivity measurements do not confirm the interstitial activation energy by Bonnecaze. Rather we determine a smaller activation energy of $E_{a,i} = 5.2\,\mathrm{kJ \cdot mol^{-1}}$ [20].

Assuming that $Q^*_i = E_{a,i}$ and $Q^*_v = E_{a,v}$, the sum $0.8 \cdot Q^*_i - 0.2 \cdot Q^*_v$ in eqn (40) equals a value of 17.2 kJ/mol (using the data by Bonnecaze) which is obviously in complete disagreement with our experiments. We, therefore, conclude that our experimental results do not support the idea of an identity between the heat of transport of point defects and their activation energy. Assuming $U^*_i = E_{a,i}$ and $U^*_v = -E_{a,v}$, i.e. identifying the energies of transport with the activation energies, the sum $0.8 \cdot U^*_i - 0.2 \cdot U^*_v$ in eqn (41) equals also 17.2 kJ/mol (using Bonnecaze's data). Thus, there is also no agreement with our experimental result.

However, we find a rough agreement between our experimental results and the assumptions $U^*_i = -E_{a,i}$ and $U^*_v = E_{a,v}$. Inserting our own value for the interstitial activation energy and using the vacancy activation energy of Bonnecaze, the sum $0.8 \cdot U^*_i - 0.2 \cdot U^*_v$ equals $-10.9\,\mathrm{kJ \cdot mol^{-1}}$ which is not too different from the experimental result in eqn (41). This agreement may be a mere coincidence and, therefore, we will not stress it. Especially as there are now theoretical reasons to doubt the existence of any direct connection between Q^* and E_a^+.

The strong increase of the heat of transport with increasing EMF is due to the term $[\alpha_e(\psi_e - 1)/((\alpha_e + \alpha_e^{-1})(1 + \alpha_e^2\psi_e))] \cdot \Delta H_e$ in the expression for $Q^*_{e^-}$, see

*In [13], Bonnecaze *et al.* evaluate a wrong activation energy for the vacancy migration. They observe two linear regions with different slope in their Arrhenius plot of the (logarithmic) ionic conductivity vs $1/T$. They assign intrinsic (interstitial-type) conductivity to the high temperature region and identify the corresponding slope correctly as $E_{a,i} + \Delta H_F/2$. Extrinsic (vacancy-type) conductivity is assigned to the low temperature region and the corresponding slope is erroneously identified with a term $E_{a,v} + \Delta H_F/2$, resulting in a negative value for $E_{a,v}$. Correctly, the slope of the extrinsic branch has to be identified directly with the vacancy activation energy and thus the vacancy activation energy equals $E_{a,v} = 33.8\,\mathrm{kJ/mol}$.

eqn (38). At the exact stoichiometric composition this term becomes $(\psi_e - 1)/(\psi_e + 1) \cdot \Delta H_e/2$. Since ΔH_e is known much better than ψ_e, one can in principle use this relation for the determination of ψ_e from the measured heat of transport. However, the evaluation of ψ_e is very sensitive to even small errors of ΔH_e and the heat of transport at the stoichiometric composition [9]. Thus, we cannot extract a precise value for ψ_e, but estimate that it lies within the range $100 < \psi_e < 200$ which can also be seen from the fit curves in Fig. 7.

The height of the maximum of Q^*_{Ag} equals approximately 82 kJ/mol which is a value close to the enthalpy ΔH_e. According to Ref. [9], the maximum is to be found approximately at $\alpha_{e,\max} = \psi_e^{-1/4}$ with an amplitude of $(\psi_e - 1)/(1 + \psi_e^{1/2})^2 \cdot \Delta H_e$. If we assume the maximum to be situated at $\alpha_{e,\max} = 0.25$ (corresponding to the EMF $U_S = 195$ mV) in Fig. 7, we find $\psi_e \simeq 256$. Inserting this value and taking $\Delta H_e = 94.7$ kJ/mol we find an amplitude of 83.2 kJ/mol. This value coincides with the measured height of the maximum (82 kJ/mol). Thus, we conclude that the mobility ratio ψ_e is indeed relatively high and in the order of 10^2.

5.4. *Comparison with the literature*

Only a few investigations of the Soret effect in nonstoichiometric compounds are reported in the literature. So far, the study of the Soret effect in mixed conducting materials has been restricted to the systems β-$Ag_{2+\delta}S$ [33, 35, 6, 7], β-$Ag_{2+\delta}Se$ [34], CeO_{2-x} [36], $(Pu, U)O_{2\pm x}$ (e.g. [28]). The study of partial thermopowers was mainly focussed on the electronic properties, in order to determine the sign and concentration of the charge carriers. However, we are not aware of experimental studies in which, besides the partial thermopower, independent information has been obtained for the electronic entropy, as in the present study. In effect, the number of systems to which such an approach can be applied is probably very small. Partial entropies of charged particles cannot be measured, thus only the entropies of neutral components (e.g. the metal as a combination of ions and electrons) are accessible from experiments. To obtain information on the composition dependence of the partial entropy of electrons (ions), the ionic (electronic) partial entropy has to be independent of the concentration of the neutral component (i.e. the metal excess or deficit). However, the partial entropy of either electrons or ions can only be composition independent if the concentration of extrinsic defects is small in comparison to the concentration of intrinsic defects and, thus, one is restricted to almost stoichiometric systems in the case of simple binary compounds.

Honders *et al.* [37, 38] report measurements of the partial ionic and electronic thermopower for the intercalation compound Ag_xTiS_2, aiming for the determination of the ionic heat of transport. They evaluate the temperature dependence of their galvanic cell of the type $Pt|Ag|AgI|Ag_xTiS_2|Pt$ incorrectly as $F \cdot (\partial U_S/\partial T)_\delta = \bar{S}_{Ag^+} - S^\circ_{Ag}$. Consequently, from the subtraction of the ionic thermopower $F \cdot \epsilon_{Ag^+} = \bar{S}_{Ag^+} - S^\circ_{Ag} + Q^*_{Ag^+}/T$ and the presumed partial entropy, Honders *et al.* determine ionic heats of transport $Q^*_{Ag^+}$. Correctly, the temperature dependence of the EMF is determined by the metal entropy $\bar{S}_{Ag} - S^\circ_{Ag}$ and, thus, it is in principle impossible to determine ionic heats of transports exclusively from experiments.

In view of the results of the present study, the low-temperature phase of silver selenide, α-$Ag_{2+\delta}Se$ is another interesting candidate for an experimental study of the nonisothermal transport properties. The situation is reversed with respect to the electronic and ionic defect structure. In contrast to the sulphide, $Ag_{2+\delta}Se$ has a smaller band gap and, thus, by changing the silver excess the electronic transport properties remain nearly constant while now the ionic defect concentration can be changed significantly. Experimental work on this system is in progress.

Another mixed conducting binary compound which can be prepared either hypo- or hyperstoichiometric is uranium dioxide, UO_{2+x}. Due to its technological relevance, various studies of thermal diffusion in this material have been performed, particularly in the 1960s and 1970s [28]. Though the experimental results in terms of the heat of transport of the oxygen component, Q^*_O, are not always convincing, the existing results indicate a strong minimum of the heat of transport near the stoichiometric composition. To date, no explanation for this observation has been given. In the light of the present study this minimum not only appears reasonable, rather one has to conclude that it is a necessary consequence of the electronic and ionic defect structures.

6. CONCLUSIONS

From measurements of the partial entropy and the entropy of transport of silver in α-$Ag_{2+\delta}S$, the heat of transport Q^*_{Ag} of silver metal has been determined for the whole range of composition at three different temperatures. In addition, the partial electronic and ionic thermopower has been measured, in order to demonstrate the separate contributions of both charge carriers to the transport properties of the metal component. As expected, the ionic thermopower remains constant throughout the whole range of composition,

whereas the electronic thermopower shows a strong composition dependence. This dependence can be interpreted within the model of a non-degenerate semiconductor. The measured entropy of transport of the silver metal shows the same composition behaviour as the electronic thermopower, as one would expect for a system with composition-independent ionic transport properties.

A strong increase of the heat of transport of the electronic charge carriers is observed in the vicinity of the stoichiometric composition. This increase reflects a maximum of the electronic heat of transport Q_e^*- in the region of intrinsic defect concentrations which is due to the influence of the local electronic defect equilibrium ($e' + h^{\cdot} = 0$). The shape and amplitude of this maximum is determined by the electron-hole formation enthalpy ΔH_e and the mobility ratio ψ_e.

In accord with previous considerations [9] it is difficult to obtain reliable quantitative information on the absolute heats of transport of mobile defects. The heats of transport of ions and electrons are complicated combinations of several independent defect quantities. Thus, in addition to the non-isothermal transport properties, isothermal transport properties like mobility ratios and the defect concentrations have to be known precisely. In the present case, we have to assume values for the heat of transport Q_n^* of the electronic defects (i.e. their kinetic energy terms), according to the most probable scattering mechanism, to obtain the ionic heat of transport.

Analysing the different contributions to $Q^*_{Ag^+}$, we obtain the sum of the heats of transport of interstitials and vacancies as $0.8 \cdot Q_i^* - 0.2 \cdot Q_v^* = -78.4\,\mathrm{kJ/mol}$. This result gives no evidence for a close relation between the heats of transport of ionic defects and their activation energy ($E_{a,i} = 5.2\,\mathrm{kJ \cdot mol^{-1}}$, $E_{a,v} = 33.8\,\mathrm{kJ \cdot mol^{-1}}$). A different conclusion can be drawn with respect to the energies of transport U_j^*: if we assume the relations $U_i^* = -E_{a,i}$ and $U_v^* = E_{a,v}$ we find an agreement between the measured heat of transport and the activation energies of interstitials and vacancies. However, in the present state of knowledge, this result may be a mere coincidence without any physical meaning and should not be taken too seriously.

Finally, it seems desirable to investigate a comparable system with composition-independent electronic properties, but variable ionic transport properties. In this case, an extremum for the heat of transport of the mobile component, being due to an ionic defect equilibrium, should be observed.

Acknowledgements—We thank H. Schmalzried for the thorough and critical reading of the manuscript and for valuable comments. This study was funded by the Deutsche Forschungsgemeinschaft (DFG) in the framework of the Sonderforschungsbereich 173 at the Universität Hannover.

REFERENCES

1. Allnatt, A. R. and Lidiard, A. B., *Atomic Transport in Solids*. Cambridge University Press, Cambridge 1993.
2. deGroot, S. R. and Mazur, P., *Non-Equilibrium Thermodynamics*. North-Holland, Amsterdam 1962.
3. Smith, R. A., *Semiconductors*, 2nd edn, p. 151. Cambridge University Press, Cambridge 1978.
4. Madelung, O., In: *Physical Chemistry, An Advanced Treatise*, Vol. 10, Academic Press, New York, Chapter 6 (ed. W. Jost) 1970.
5. Janek, J., *Ber. Bunsenges. Phys. Chem.*, 1995, **99**, 920.
6. Janek, J. and Korte, C., *Ber. Bunsenges. Phys. Chem.*, 1995, **99**, 932.
7. Korte, C. and Janek, J. *Ber. Bunsenges. Phys. Chem.*, 1996, **100**, 425.
8. Wever, H., *Elektro- und Thermotransport in Metallen*. Johann Ambrosius Barth, Leipzig 1973.
9. Janek, J. and Korte, C., *Z. Phys. Chem.* 1996, 196.
10. Schmalzried, H., *Progr. Solid St. Chem.*, 1980, **13**, 119 .
11. Reye, H. and Schmalzried, H., *Z. Phys. Chem. N. F.*, 1981, **128**, 93.
12. Valverde, N., *Z. Phys. Chem. N. F.*, 1970, **70**, 113.
13. Bonnecaze, G., Lichanot, A. and Gromb, S., *J. Phys. Chem. Sol.*, 1978, **39**, 299.
14. Lazzari, M., Bicelli, L. P., Razzani, G., Rivolta, B. and Romagnani, C., *Gazz. Chim. Ital.*, 1974, **104**, 139.
15. Weiss, K., *Z. Naturforsch.*, 1969, **24a**, 184.
16. Junod, P., *Helv. Phys. Acta*, 1959, **22**, 567.
17. Becker, K.-D., Schmalzried, H. and von Wurmb, V., *Solid State Ionics*, 1983, **11**, 213.
18. Ding, S. and Petuskey, W. T., *Solid State Ionics*, 1992, **58**, 123.
19. Brüesch, P. and Wullschleger, J., *Solid State Comm.*, 1973, **13**, 9.
20. Korte, C., Ph. D. thesis (in preparation).
21. Wagner, C., *Progr. Solid St. Chem.*, 1972, **7**, 1.
22. Sugisaki, M., Sato, S. and Furuya, H., *J. Nucl. Mater.*, 1981, **97**, 79.
23. Becker, R., *Theorie der Wärme*, Springer, Heidelberg, 1985, p. 125.
24. Becker, J. H. and Frederikse, H. P. R., *J. Appl. Phys.*, 1962, **33**(1), 447.
25. Rickert, H., *Electrochemistry of Solids*, Springer, Heidelberg, 1982.
26. Magistris, A., Pezzati, E. and Sinistris, C., *Z. Naturforsch.*, 1972, **27a**, 1379–1381.
27. Shahi, K. and Chandra, S., *Z. Naturforsch.*, 1975, **30a**, 1055.
28. Kamata, M. and Esaka, T., *J. Appl. Electrochem.*, 1994, **24**, 390.
29. Kubaschewsky, O., Alcock, C. B. and Spencer, P. J., *Materials Thermochemistry*, 6th edn. Pergamon Press, New York, 1993.
30. Korte, C. and Janek, J., *Solid State Ionics* (1996) (in press).
31. Jost, W. and Kubaschewski, P., *Z. Phys. Chem. N. F.*, 1968, **60**, 69.
32. Allnatt, A. R. and Chadwick, A. V., *Chem. Rev.*, 1967, **67**, 681.
33. Rickert, H. and Wagner, C., *Ber. Bunsenges. Phys. Chem.*, 1963, **67**, 621.
34. Koch, W., Rickert, H. and Schlechtriemen, G., *Solid State Ionics*, 1983, **9/10**, 1197.
35. Miyatani, S., *J. Phys. Soc. Jpn.*, 1968, **24**, 328.
36. Millot, F. and Gerdanian, P., *J. Nucl. Mater.*, 1983, **116**, 55.
37. Honders, A., Young, E. W. H., de Wit, J. H. W. and Broers, G. H. J., *Solid State Ionics*, 1983, **8**, 115.
38. Honders, A., Hintzen, A. J. H., der Kinderen, J. M., de Wit, J. H. W. and Broers, G. H. J., *Solid State Ionics*, 1983, **9 & 10**, 1205.

39. Reye, H., *Z. Phys. Chem. N. F.*, 1980, **119**, 251.
40. Wagner, C., *J. Chem. Phys.*, 1953, **21**(10), 1819.
41. Wagner, C., *Progr. Solid State Chem.*, 1971, **6**, 1.
42. Schmalzried, H., *Ber. Bunsenges. Phys. Chem.*, 1983, **87**, 726.

APPENDIX

Coulometric titration of α-Ag_2S

The original derivation of the formal relation between the composition of $Ag_{2+\delta}S$ and the silver activity, i.e. the EMF of a coulometric titration cell, has been given by Wagner [40]. Further details can be found e.g. in Refs [41, 42]. Only a short summary is given here for the sake of completeness and since we need information on the temperature dependence of the EMF at the stoichiometric composition. In accord with eqns (1) and (2) we can write (under the assumption of an ideal solution of point defects)

$$K_F = x_i \cdot x_v \qquad K_e = x_n \cdot x_n \tag{A1}$$

with x denoting molar fractions $x_j = c_j \cdot V_m$. With

$$\delta = x_n - x_p \tag{A2}$$

and the definitions

$$\alpha_e \equiv x_n/x_n^{\#} \qquad \alpha_e^{-1} \equiv x_p/x_p^{\#} \tag{A3}$$

one obtains

$$\delta = \sqrt{K_e}(\alpha_e - \alpha_e^{-1}).$$

To obtain x_n and x_p as a function of δ, eqn (A1) has to be written as:

$$K_e = x_n \cdot x_p = (x_n^{\#} + \delta - x)(x_p^{\#} - x) \tag{A4}$$

with x denoting the molar fraction of holes and electrons which will disappear or appear by recombination or formation of electrons and holes. Solving this equation for x and reinsertion yields the desired expressions:

$$\ln\frac{x_n}{x_n^{\#}} = \operatorname{arsinh}\left(\frac{\delta}{2\sqrt{K_e}}\right) = \ln\alpha_e \tag{A5}$$

$$\ln\frac{x_p}{x_p^{\#}} = \operatorname{arsinh}\left(-\frac{\delta}{2\sqrt{K_e}}\right) = \ln\alpha_e^{-1}. \tag{A6}$$

The EMF of the cell Pt/Ag/α-AgI/Ag_2S/Pt is determined by the difference of the chemical potentials of silver in the sulphide and the pure silver electrode:

$$-FU = \mu_{Ag} - \mu_{Ag}^{\circ} = RT\ln a_{Ag}. \tag{A7}$$

The chemical potential of the silver component in the sulphide equals the sum of the chemical potentials of the respective building units:

$$\mu_{Ag} = \mu_{Ag^+} + \mu_{e^-} = \mu_i + \mu_n = -(\mu_v + \mu_p) \tag{A8}$$

i.e.

$$a_{Ag} = a_i \cdot a_n \simeq x_i \cdot x_n. \tag{A9}$$

Assuming that the Frenkel equilibrium is not disturbed by changes of δ in the whole range of composition, $x_i \approx x_v \approx x_i^{\#} = x_v^{\#}$, the relation

$$-\frac{F(U - U^{\#})}{RT} = \ln\alpha_e \tag{A10}$$

follows from a combination of eqns (A3), (A7) and (A9) with $-FU^{\#} = RT\ln x_i^{\#}x_n^{\#}$. Combining eqns (A5) and (A10), one ends with

$$U - U^{\#} = -\frac{RT}{F}\operatorname{arsinh}\left(\frac{\delta}{2\sqrt{K_e}}\right) \tag{A11}$$

with $U^{\#}$ denoting the EMF at the stoichiometric composition. Differentiating eqn (A11) by dT and taking the temperature dependence of K_e and $U^{\#}$ into account, it follows an expression for the (relative) partial molar entropy of silver:

$$\begin{aligned} F\left(\frac{\partial U}{\partial T}\right)_{\delta} &= R\left[\frac{\Delta H_e^{\circ}}{2RT}\tanh(\ln\alpha_e) - \ln\alpha_e\right] \\ &\quad + F\left(\frac{\partial U^{\#}}{\partial T}\right)_{\delta} \\ &= F\left[\frac{\partial(\mu_{Ag} - \mu_{Ag}^{\circ})}{\partial T}\right]_{\delta} = \bar{S}_{Ag} - S_{Ag}^{\circ}. \end{aligned} \tag{A12}$$

A comparison of this expression with the partial entropy of electrons (eqn (36)) finally leads to the relation

$$F\left(\frac{\partial U^{\#}}{\partial T}\right)_{\delta=0} = (\bar{S}_{Ag^+} - S_{Ag}^{\circ}) + \frac{3}{4}R\ln\frac{m_n^*}{m_p^*}. \tag{A13}$$

Thus, $U^{\#}$ is temperature dependent. From a measurement of this dependence, one can determine either the effective mass ratio m_n^*/m_p^* or the partial ionic entropy $\bar{S}_{Ag^+}$, once the other quantity is known.

According to eqn (A12) and (A13), the partial molar entropy attains a limiting slope of $-R$ at small or large values for α_e, if $\bar{S}_{Ag} - S_{Ag}^{\circ}$ is plotted vs $\ln\alpha_e$. The entropy curve has an inflection point at the stoichiometric composition $\delta = 0$ ($x_n^{\#} = x_p^{\#}$ and $\ln\alpha_e = 0$) with the slope $\Delta H_e^{\circ}/2T - R$. The entropy difference $\Delta(\bar{S}_{Ag} - S_{Ag}^{\circ})_{max}$ between the both extrema equals

$$\begin{aligned} \Delta(\bar{S}_{Ag} - S_{Ag}^{\circ})_{max} &= R\left[\left(\frac{\Delta H_e^{\circ}}{RT} - 2\right)\right. \\ &\quad \left. - \ln\left(\frac{\Delta H_e^{\circ}}{RT} - 1\right)\right] \simeq \Delta H_e^{\circ}/T \end{aligned} \tag{A14}$$

and can be approximated as $\Delta H_e^{\circ}/T$ if $\Delta H_e^{\circ}/RT \gg 1$.